16th European Symposium on Computer Aided Process Engineering
and 9th International Symposium on Process Systems Engineering
W. Marquardt, C. Pantelides (Editors)

Optimization studies in sulfuric acid production

Anton A. Kiss,[a] *Costin S. Bildea,*[b] *Peter J.T. Verheijen*[b]
[a] *University of Amsterdam, Nieuwe Achtergracht 166, 1018 WV Amsterdam, The Netherlands*
[b] *Delft University of Technology, Julianalaan 136, 2628 BL Delft, The Netherlands*

1. Abstract

Current legislation imposes tighter restrictions to reduce the impact of process industry on environment. This work presents the dynamic simulation and optimization results for an existing sulfuric acid plant. Operational problems may occur when the process is disturbed due to production rate changes or catalyst deactivation, the non-linear response of the plant leading to sustained oscillations. Since the plant is operated near full capacity, only minor increases in energy production can be achieved. However, the SO_x emissions can be significantly reduced by ~40% or more, by optimizing the operating parameters.

2. Introduction

Most sulfuric acid plants are rather old and are facing now additional challenges that aim to maximize the amount of energy produced while reducing the environmental impact. Sulfuric acid is the chemical product manufactured in largest quantity in terms of mass, with about 40 million tons produced annually only in USA. It has a wide range of uses and plays an important role in the production of almost all manufactured goods. Approximately 65% of the H_2SO_4 produced is used in the production of agricultural fertilizers.

This study presents the results of the dynamic simulation and optimization of an existing sulfuric acid plant (PFI – *Phosphoric Fertilizers Industry*, Greece). Due to the partnership with *Process Systems Enterprise Ltd.* (PSE), and thanks to its powerful features, *g*PROMS was selected to perform all simulation tasks.[1] The dynamic model developed in this study includes also a graphical user interface (GUI) built in MS Excel, that allows scenario evaluation and operator training. The model has been successfully used for dynamic simulations to evaluate the non-steady-state behavior of the plant and detect changes in product quality, as well as to minimize the total amount of sulfur oxides released in atmosphere.

For the major units of the flowsheet, the main equations describing the dynamic model are given using the standard notation. Due to space limitations and model complexity, some modeling details were omitted but they are available upon request. Here we limit to present only the most important results of this study.

3. Process description

The main steps in this process consist of burning sulfur (S) in air to form sulfur dioxide (SO_2), converting SO_2 to sulfur trioxide (SO_3) using oxygene (O_2) from air, and absorbing the sulfur trioxide in water (H_2O) or a diluted solution of sulfuric acid (H_2SO_4) to form a concentrated solution of acid (>96%).
Because the reaction is limited by the chemical equilibrium a multi-bed catalytic adiabatic reactor is used. The catalyst used is vanadium oxide (V_2O_5) mixed with an alkali metal sulfate. This mixture is supported on small silica beads, and it is a liquid at the high temperature inside the reactor.
Several conversion steps, addition of fresh air and inter-stage cooling are necessary as the reaction is reversible and exothermal.[2] For heat integration reasons, two feed-effluent heat exchangers (FEHE) are used. SO_2 conversion is further improved and tail gas emissions are reduced through an intermediate SO_3 absorption step. The absorption of SO_x is finalized in the second absorber.
The simplified flowsheet of the sulfuric acid production process consists of a sulfur burner, multi-pass converter, heat exchangers and absorbers (Figure 1). The process is designed to give a conversion of sulfur dioxide to sulfuric acid of over 99.7%. This is achievable in practice due to the intermediate absorption (after the fourth bed of catalyst) that changes the gas composition, thus shifting the equilibrium curve to higher conversions (Figure 2).
The model parameters were measured or estimated using standard correlations.

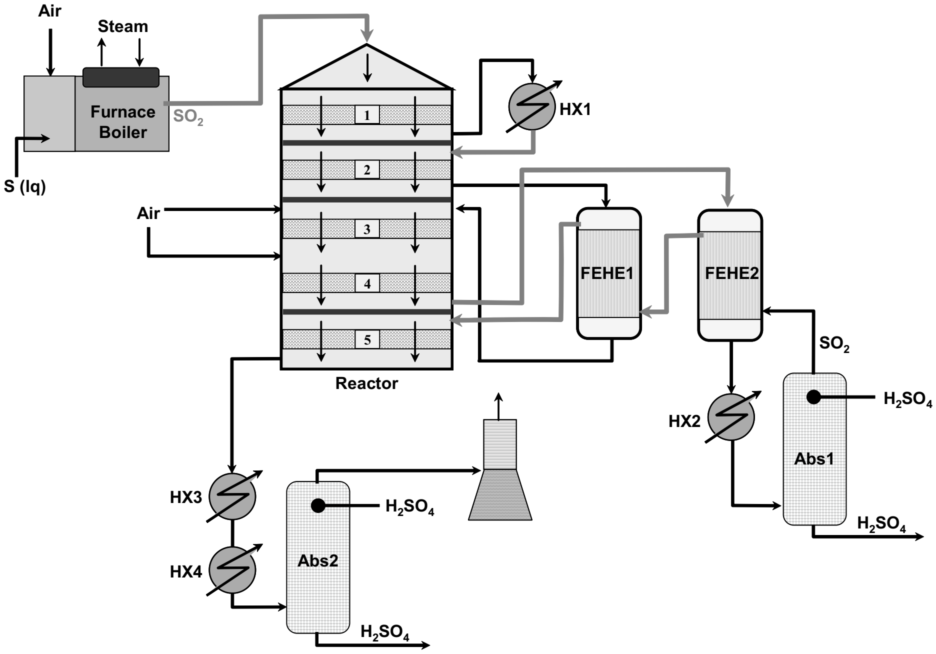

Figure 1. Simplified flowsheet of sulfuric acid production plant.

Dynamic model

1. Oxidation reactor (multi-pass adiabatic converter, five beds of catalyst)

Mass balance:
$$\frac{dc_i}{dt} = -u\frac{dc_i}{dz} + \rho_b \cdot \nu_i \cdot r + D_z\frac{d^2c_i}{dz^2} \qquad (1)$$

Energy balance:
$$\left(\varepsilon \cdot \rho_f \cdot c_{p,f} + \rho_b \cdot c_{p,cat}\right)\cdot\frac{dT}{dt} = -\rho_f \cdot c_{p,f} \cdot u\frac{dT}{dz} + \rho_b \cdot r \cdot \left(-\Delta H_r\right) + k_z\frac{d^2T}{dz^2} \qquad (2)$$

Pressure drop:
$$\frac{dP}{dz} = -f_f \cdot \rho_f \cdot \frac{u^2}{D_p} \qquad (3)$$

A kinetic model similar to the one proposed by Froment & Bischoff was used:[2]

$$r = \frac{k_1 \cdot p_{\mathrm{O_2}} \cdot p_{\mathrm{SO_2}} \cdot \left(1 - \dfrac{p_{\mathrm{SO_3}}}{K_p \cdot p_{\mathrm{SO_2}} \cdot p_{\mathrm{O_2}}^{1/2}}\right)}{22.414 \cdot \left(1 + K_2 \cdot p_{\mathrm{SO_2}} + K_3 \cdot p_{\mathrm{SO_3}}\right)^2} \qquad (\text{kmol/kg·cat·s}) \qquad (4)$$

where $K_p = \exp\left(\text{-10.68 } + 11300/\mathrm{T}\right)$ and $k_1 = k_{1,0} \cdot \exp\left(-E_{\mathrm{a,1}}/T\right)$ (5)

2. Heat exchangers (HEX with constant coolant temperature and FEHE)

Energy balance (HEX):
$$\rho_f \cdot c_{p,f} \cdot \frac{dT}{dt} = -\rho_f \cdot c_{p,f} \cdot u\frac{dT}{dz} - \frac{4}{D} \cdot H_w \cdot \left(T - T_c\right) \qquad (6)$$

Energy balance (FEHE):
$$\frac{dT_1}{dt} = -u_1\frac{dT_1}{dz} - \frac{4}{D} \cdot \frac{H_w}{\rho_1 \cdot C_{p,1}}\left(T_1 - T_2\right) \qquad (7)$$

$$\frac{dT_2}{dt} = u_2\frac{dT_2}{dz} + A_v \cdot \frac{H_w}{\rho_2 \cdot C_{p,2}}\left(T_1 - T_2\right) \qquad (8)$$

3. Absorbers (A – SO_3 in gas phase; B – H_2O in liquid phase)

Mass balance gas (A):
$$\varepsilon_G \cdot \frac{dc_{\mathrm{A}}}{dt} = -\frac{4}{\pi \mathrm{D}^2}\frac{d}{dz}\left(F_G \cdot C_{\mathrm{A}}\right) - N_{\mathrm{A}} \cdot A_v \qquad (9)$$

Mass balance liquid (B):
$$\varepsilon_L \cdot \frac{dc_{\mathrm{B}}}{dt} = -\frac{4}{\pi \mathrm{D}^2}\frac{d}{dz}\left(F_L \cdot C_{\mathrm{B}}\right) - N_{\mathrm{B}} \cdot A_v \qquad (10)$$

Energy balance (gas):
$$\varepsilon \cdot \frac{dT_1}{dt} = -\frac{4}{\pi D^2} \cdot F_G\frac{dT_1}{dz} - \frac{H_w \cdot A_v}{\rho_G \cdot c_{p,G}}(T_1 - T_2) \qquad (11)$$

Energy balance (liquid):
$$\left(1 - \varepsilon\right) \cdot \frac{dT_2}{dt} = \frac{4}{\pi D^2} \cdot F_L\frac{dT_2}{dz} + \frac{H_w \cdot A_v}{\rho_L \cdot c_{p,L}}(T_1 - T_2) + \frac{N_A \cdot A_v}{\rho_L \cdot c_{p,L}} \cdot \left(-\Delta H_R\right) \qquad (12)$$

Pressure drop:
$$\frac{dP}{dz} = -f_f \cdot \rho_f \cdot \frac{u^2}{D_p} \qquad (13)$$

Note**:** The standard notation was used in describing the model equations (Eq. 1-13).

4. Results and discussion

The path of the reaction can be conveniently shown in the *X–T* diagram (Figure 2). The horizontal lines represent gas cooling only, as no conversion occurs when the gas is not in contact with the catalyst. The diagonal lines represent adiabatic temperature rise of the gas within the different converter passes. Their slopes are directly proportional to the specific heat capacity of the gas. Each initial gas concentration of SO_2 has its own equilibrium curve. For a given gas composition, the adiabatic temperature-rise can approach the equilibrium curve but never cross it.

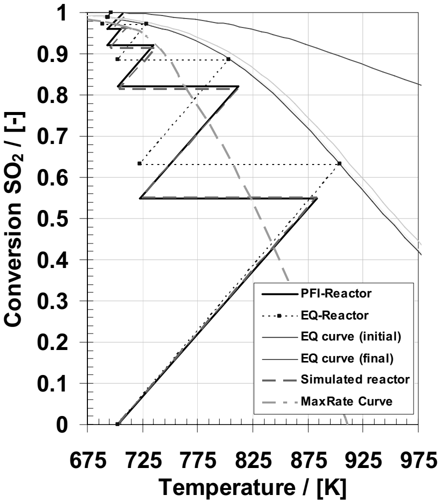

Figure 2. Temperature-conversion diagram.

Operational problems may occur when the process is disturbed due to production rate changes, catalyst deactivation, or variation of air feed flow rates caused by day-night or summer-winter temperature differences and constant volumetric flow operation. For certain disturbances (–5% feed flow rate), the response of the plant is nonlinear and leads to sustained oscillations (Figure 3). Obviously, these oscillations are not acceptable since they propagate from the reactor to absorbers, rendering the plant unstable and the product off-spec. The non-linear behaviour is explained by the presence of an inverse response[3] for the temperature through the reactor beds, combined with the positive energy feedback induced by the two feed-effluent heat exchangers (FEHE).

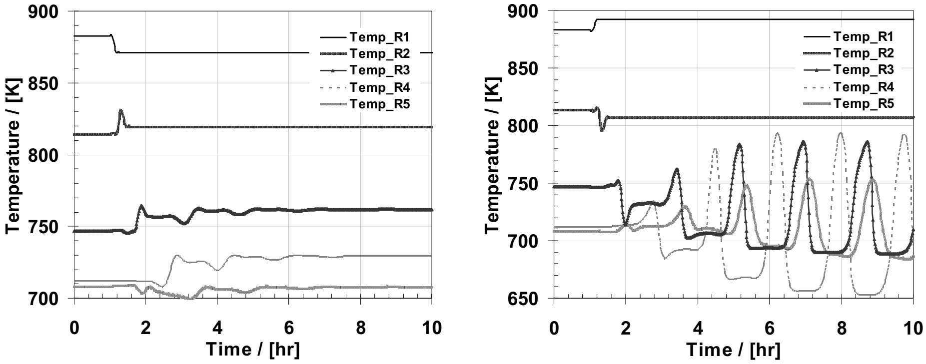

Figure 3. Reactor temperatures time-profile, for ± 5% change in air feed flow rate (initial case).

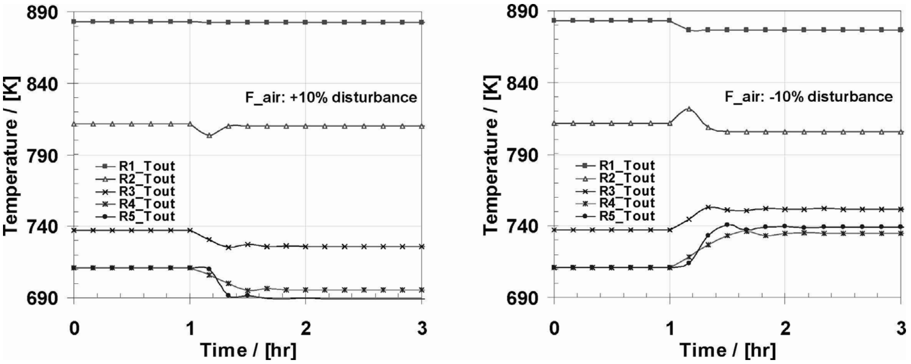

Figure 4. Reactor temperatures time-profile, for ± 10% changes in air feed flow rate (final case).

The plant can be stabilized by changing the catalyst distribution among the conversion stages (e.g. shortening the length of several catalyst beds) and employing feedback temperature controllers. By applying these changes to the reactor, the sustained oscillations are avoided and the dynamic response becomes acceptable even for larger disturbances in the feed flow rate (Figure 4). The molar fractions of SO_2 and SO_3 at the outlet of the final absorption column, are presented for similar disturbances in Figure 5. Note the non-symmetrical response (–50%...+200% for SO_2) to these ±10% disturbances. However, the composition reaches a new steady state in relatively short time, less than 1 hour.

Multi-variable optimization was performed for several production rates, corresponding to the amount of sulfur fed into the plant (nominal value and ± 5-10% changes). Five key variables were identified and manipulated accordingly to carry out the optimization: the amount of air fed into the sulfur burner, the flow rates of air fed into converter pass 3 and 4, and split fractions (by-pass) for cold streams entering the gas-gas heat exchangers (FEHE1 and FEHE2). In both optimizations the cold streams should not be split to bypass the heat exchangers.

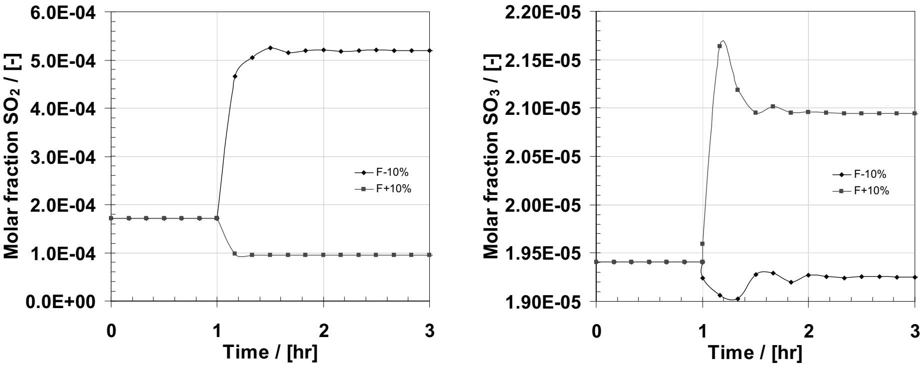

Figure 5. Molar fractions of SO_x after absorption, for ± 10% disturbance in the air feed flow rate.

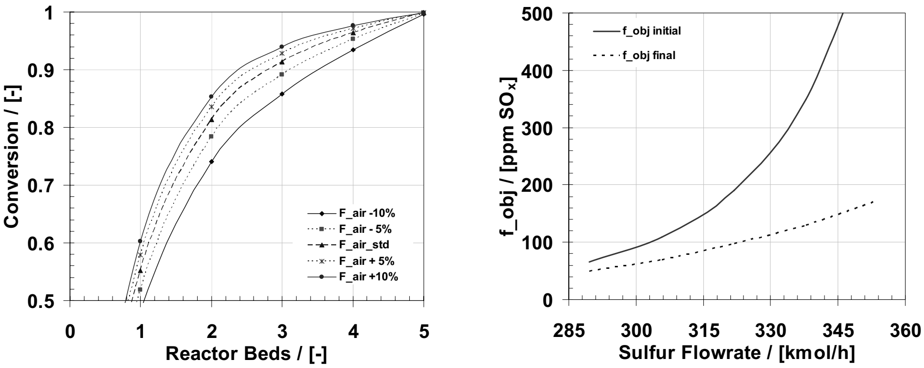

Figure 6. Conversion profiles in the reactor, for ± 10% changes in the air feed flow rate (left). SO_x emissions (lower is better) before and after optimization at various feed flow rates (right).

The optimization targets were to maximize the amount of energy produced, and minimize the total amount of SO_x released in atmosphere (*i.e.* not absorbed in the final absorption column). The conversion profiles in the reactor for changes of ± 10% in the feed flow rate are given in Figure 6 (left). Increasing energy production is equivalent to maximizing the amount of SO_2 converted into products. A flat optimum is expected, since the heat generated in the reaction is the one that is recovered. As the conversion of the process is almost 99.85%, any further increase is insignificant. Not surprinsingly, the energy production can be increased by only ~1%. However, the SO_x emissions can be drastically reduced by ~40% (the nominal case) or even more (Figure 6, right). Therefore, the plant can be fully exploited while respecting the ecological restrictions.

5. Conclusions

The dynamic model developed in this work provides reliable results that are in excellent agreement with the data available from the real plant, the relative error being typically less than 1%. Along with minor benefits in energy production the amount of SO_x emissions could be significantly reduced by ~40% just by optimizing operating parameters such as feed flow rates or split fractions. Besides controllability, operability and optimization studies the plant model coded in *g*PROMS is also useful for operator training and scenario assessments.

Acknowledgement. This project (OPT-ABSO, Contract nr. G1RD-CT-2001-00649) was funded by the European Commission. We also thank PFI and PSE for assistance.

References

1. gPROMS Advanced User Guide, Process Systems Enterprise Ltd., 2004.
2. Froment, G.F., Bischoff, K.B., Chemical Reactor Analysis and Design, Wiley, 1979.
3. Morud J.C. and Skogestad S., AIChE Journal, 1998, 44, 888.